The submitted manuscript has been authored by a contractor of the U. S. Government under contract No. W-31-109-ENG-38. Accordingly, the U. S. Government retains a nonexclusive, royalty-free license to publish or reproduce the published form of this contribution, or allow others to do so, for U. S. Government purposes.

ANL/TD/CP--88550

CONF-960443--1

AEROSOL MEASUREMENTS FROM PLASMA TORCH CUTS ON STAINLESS STEEL, CARBON STEEL, AND ALUMINUM*

Vincent J. Novick, Christie-Joy Brodrick, Sheila Crawford, James Nasiatka, Kathleen Pierucci, Vincent Reyes,
James Sambrook, Stanley Wrobel, John Yeary
Technology Development Division
Argonne National Laboratory
9700 S. Cass Ave.
Argonne, Illinois, 60439
(708) 252-6629

RECEIVED
JAN 11 1995
OSTI

ABSTRACT

The main purpose of this project is to quantify aerosol particle size and generation rates produced by a plasma torch when cutting stainless steel, carbon steel and aluminum. The plasma torch is a common cutting tool used in the dismantling of nuclear facilities. Eventually, other cutting tools will be characterized and the information will be compiled in a user guide to aid in the planning of both D&D and other cutting operations. The data will be taken from controlled laboratory experiments on uncontaminated metals and field samples taken during D&D operations at ANL nuclear facilities.

The plasma torch data was collected from laboratory cutting tests conducted inside of a closed, filtered chamber. The particle size distributions were determined by isokinetically sampling the exhaust duct using a cascade impactor. Cuts on different thicknesses showed there was no observable dependance of the aerosol quantity produced as a function of material thickness for carbon steel. However, data for both stainless steel and aluminum revealed that the aerosol mass produced for these materials appear to have some dependance on thickness, with thinner materials producing more aerosols. The results of the laboratory cutting tests show that most measured particle size distributions are bimodal with one mode at about 0.2 µm and the other at about 10 µm. The average Mass Median Aerodynamic Diameters (MMAD's) for these tests are 0.36±0.08 µm for stainless steel, 0.48±0.17 µm for aluminum and 0.52±0.12 µm for carbon steel.

INTRODUCTION

Decontamination and Decommissioning (D&D) operations mark the end of a nuclear facility's effective service life. A major portion of the decommissioning effort is the disassembly of structural components. Generally, these structures must be assumed to be either radioactive or contaminated, presenting unique personal and environmental hazards when planning for their disassembly. The potential for exposure to whole body doses of radiation requires that the disassembly operations be performed as fast as possible. However, the fastest cutting tools generally produce more aerosols, noxious gases, and secondary waste. Clearly, the need to reduce one hazard must be weighed against the creation of additional hazards generated by different cutting techniques. Since the main hazard of cutting is the generation and release of potentially contaminated airborne particles, it is important to have a clear understanding and quantification of the aerosols produced by various cutting tools. This problem has been addressed by various researchers around the world (1-7). This work attempts to expand upon their work of attempting to quantify some of the potential hazards from D&D cutting operations. In particular, it is planned to expand the efforts of Bach (1) to compile cutting information into a computerized user guide for contractor reference.

In addition to simply including data in a database, the proposed user guide is expected to be a resource that can furnish a D&D project with guidelines in terms of predicting total aerosol production, aerosol generation rates, suggested tool operating settings, and the minimum HEPA filtration area necessary to contain the expected aerosol release. D&D contractors, planners, and ES&H personnel will be able to use this information in conjunction with the specifics of the application and site specific safety guidelines, to determine the appropriate cutting tool for the job, and the necessary pollution controls required, including filtering, personal protection, and air monitoring. It may also assist in the selection of an appropriate cutting tool and recommend cutting speeds or other pertinent tool parameters.

In order to provide an empirical prediction of the aerosol quantity produced, a testing plan, consistent with the principles of risk assessment, was devised to determine the worst case scenario in terms of maximum aerosol production for a given material. This was done by determining the cutting torch power that maximized aerosol production, then varying the cutting speed at that power to determine the parameters that produced the maximum mass of aerosols. Once these parameters were defined, varying length cuts were made on samples of different thicknesses and the quantity of aerosols generated was plotted against the length of cut multiplied by the thickness of the material. The first phase of this work focused on laboratory tests using a 100 A plasma torch (ESAB Welding Products model PCS-100) in an experimental chamber, to cut flat plates of carbon steel, stainless steel and aluminum. In

DISTRIBUTION OF THIS DOCUMENT IS UNLIMITED

MASTER

addition to the laboratory test results and observations, this work also reports some limited field sampling data.

Plasma Torch Cutting

The plasma arc torch has the capability of cutting any conductive material by melting and vaporizing the material in the area being cut. The torch operates by creating a direct current arc between a tungsten electrode and the metal workpiece. Since plasma temperatures reach 20,000 to 40,000 degrees Celsius, a small portion of the metal workpiece is melted. The molten metal is then blown away by compressed air or other gas. As the torch is moved relative to the workpiece, a kerf or cut is created in the piece.

A plasma torch cut produces particles by condensation of metal vapors, and droplet formation from liquid metal shear forces. Condensation occurs when the vaporized metal diffuses away from the workpiece and cools, resulting in the nucleation of aerosol particles. These nucleation particles can continue to grow as additional vapor condenses, but typically remain smaller than 1 μm in diameter. In general, when the temperature of the cut is increased due to higher energy inputs, the quantity and size of the aerosols produced through the vaporization and condensation mechanism will increase.

The droplet method of aerosol production occurs as the molten metal is blown from the workpiece with the compressed gas flowing through the torch, forming the kerf. The molten metal forms droplets due to the liquid metal shear forces as the compressed gas forces the liquid metal from the kerf. This mechanism of droplet formation is referred to as atomization. As the droplets are blown from the cut, larger drops immediately fall to the bottom of the chamber and contribute to the dross or secondary waste generated by the cutting process. Smaller droplets are entrained by the gas flow and can remain suspended in the cutting chamber for long periods of time. These droplets cool rapidly and form aerosols much larger in size than those generated by condensation mechanisms.

The relationship between the cutting parameters and the quantity and size distribution of the aerosols produced by a cut is more easily understood by considering the energy input into the workpiece. Energy is defined as the integral of the power as a function of time. Electrical power is the product of the current and voltage. Because the experimental apparatus maintains a constant torch height above the workpiece and it is assumed that the arc resistance is a function of the gap distance between the torch and the workpiece, we assume that the arc voltage is relatively constant. This implies that the torch power, and therefore the energy deposited into the workpiece, is a function of the current.

Furthermore, the time that the power is supplied to the workpiece is approximately equal to the cut length divided by the cutting speed. Therefore, the energy is directly related to the current and inversely related to the cutting speed.

$$E = V * I * L / R \tag{1}$$

where;

L = the length of the cut.
R = the cutting speed.

When the energy to the workpiece is increased, more material is vaporized to later condense as more and larger aerosol. Additional molten metal is also formed and made available for atomization. However, an increase in energy not only provides an increase in the amount of molten metal but also increases the width of the kerf. A wider kerf will tend to result in a decrease in the amount of atomized aerosol because of the decrease in the air velocity through the kerf. Another factor that plays a role in the quantity and size of the atomized aerosol produced, is the viscosity of the molten metal. The viscosity of the molten metal is a function of the metal and the temperature. The temperature, in turn, is a function of the energy input, the gas flow rate, the material conductivity and the thickness of the material. Both of these aerosol production processes are far to complex to model with simple equations.

Experimental Set-up

In order to maintain a controlled cutting and sampling environment, each workpiece was cut in the center of a 1.22 m x 1.22 m x 2.44 m (4 x 4 x 8 ft) box. The material was cut by moving the metal workpiece under a stationary torch. The plasma torch head was mounted to allow the height above the workpiece to be constant and reproducible regardless of the thickness of the workpiece. The fixed torch and moving workpiece geometry allowed for a consistent and stationary source of aerosols regardless of the length of the cut, in the hope of minimizing sampling errors.

Two sets of rails and carriages were utilized to move the workpiece during the cut. One pair on the floor of the box and the other pair were mounted on carriages perpendicular to the floor rails. One of the carriages supporting the workpiece was propelled by a ball screw driven by a stepper motor. The motion of the workpiece was microprocessor controlled which allowed the placement, acceleration, and velocity of the workpiece to be programmed. This allowed workpiece movements to be reproducible and precisely controlled. The workpiece was clamped onto carriages that were electrically and thermally insulated from the metal plate by ceramic spacers located between the workpiece and the carriages.

Particles and gases produced during the cutting operation were extracted from the box directly above the torch. The aerosols were sampled with a cascade impactor to measure the particle size distributions. The cascade impactor probe was fed through the center of an 11 cm (4.5") diameter elbow attached to the box. The probe was designed to take a representative sample of aerosols at 10 lpm from a total flow of 710 lpm (25 cfm) through the elbow. In most tests, a 20 cm x 20 cm x 15 cm (8" x 8" x 6") pleated HEPA glass fiber filter was attached to the other end of the elbow and collected the remaining aerosols from the box for mass analysis. A blower motor located downstream of the filter, was automatically controlled to maintain a flowrate of 710 lpm to draw the aerosols from the box, through the filter. Pressure equilibrium in the box was maintained by allowing room air to enter the box through two HEPA filters located at either end of the box. This arrangement prevented room aerosols from mixing with the aerosols generated by the cutting process and maintained the pressure in the box to within 125 Pa (0.5" H_2O) of atmospheric pressure.

Test Plan

The scope of the test plan did not allow for a detailed investigation of every variable of plasma torch operation. Therefore, the laboratory tests maintained a constant compressed gas pressure of 80 psig resulting in a gas flow rate of 144 lpm (5 cfm), the torch height was fixed so that the drag shield of the torch was about 0.025 cm above the plate being cut. The drag shield itself was designed to maintain a 0.5 cm gap between the torch nozzle and the workpiece. Preliminary scoping tests with 0.12 cm (0.046"), 0.15 cm (0.057") and 0.17 cm (0.067") torch nozzles indicated that aerosol production was not a strong function of nozzle size. Therefore, the 0.17 cm (0.067") torch nozzle, specified as an 80 amp tip, was used for most of the tests.

For each material tested, the goal was to determine the maximum amount of aerosol mass generated for typical ranges of cutting parameters subject to our equipment limitations (e.g. A maximum current of 100 A on the plasma torch power supply). The purpose was to determine a worse case scenario for aerosol release that might account for varying factors inherent in field applications, but controlled in the laboratory setting. The maximum aerosol mass production, for each material, was determined by first fixing the cutting speed and the cut length, then varying the plasma torch current. The torch current corresponding to the maximum mass of aerosol produced was then fixed and the cutting speed was varied to again determine the maximum aerosol production. The plate thickness was fixed at 0.95 cm (3/8"), after it was observed that for aluminum and stainless steel, the greatest quantity of aerosols was produced by the thinner plate thicknesses. After determining the maximum aerosol generated as a function of cutting speed and current, the speed and current were fixed and the length of the cut and thickness of the material plate were varied. The cuts were conducted on 304 stainless steel of 3/8", 1/2" and 1" thicknesses, 1018 carbon steel of 3/8" and 3/4" thickness and 6061-T6 aluminum of 3/8" and 3/4" thickness.

RESULTS

Aluminum

For aluminum, the maximum aerosol generation was found to occur at the maximum current of the plasma torch unit. Because of the torch limitations, it is not known whether this linear relationship continues or if there is a peak in aerosol production at a higher currents. A peak in aerosol production is possible if the shear force becomes too small to break up the liquid metal or if the shear force is not sufficiently large to create droplets that can be suspended in the chamber. This can occur if the increase in plasma current causes a wider kerf which would decrease the gas velocity which in turn reduces the shear forces on the molten metal. Since the atomized droplets contain more mass, less atomization will result in a decrease in aerosol mass. In fact, a peak in aerosol production was observed at a plasma current less than 100 A, but only for carbon steel.

The next set of cuts varied the cutting speed while maintaining the torch current at 100 A, the cut length at 40 cm, the same material thickness and a constant torch height above the workpiece. A maximum in aerosol generation was observed at 0.4 cm/s. A maxima in the mass of aerosol generated is expected if the same energy deposition arguments are considered. At slower cutting speeds there is more energy input to the workpiece as described by Equation 1. Aerosol production will increase with energy input until the energy input causes an increase in the kerf width which lowers the gas velocity and hence the shear force on the molten metal, at which point the aerosol mass production decreases.

After determining the cutting speed and plasma torch current for maximum aerosol generation, the length of the cut and the thickness of the material were varied. Cuts were made on 0.95 cm (3/8") and 1.9 cm (3/4") thick aluminum plates at 100 A and 0.4 cm/s, for lengths ranging from 25 to 50 cm. In addition, the test plan to determine the maximum aerosol production was repeated on the 1.9 cm (3/4") aluminum plate to determine differences in torch parameters and aerosol production rates between the two different thicknesses. The maximum aerosol production was again found at the torch limit of 100 A, but at a cutting speed of 0.125 cm/s, which was less than half of the cutting speed for the thinner plate. The aluminum test results are shown for each thickness of material as seen in Figure 1. The thinner material has the steepest slope at 317 g/m^2

compared to 15.8 g/m^2 for the 3/4" data taken at the same current and cutting speed, and a slope of 198 g/m^2 for the 1.9 cm (3/4") aluminum at 100 A and a cutting speed of 0.125 cm/s. The reason for this disparity between the thicknesses is postulated to be that the thinner material does not provide as large of a heat sink as the thicker material. As a result, the thinner material would attain higher temperatures around the kerf area and more material would be vaporized and liquified which in turn results in the production of more aerosols. The same trend of different linear relationships for each plate thicknesses was also observed for stainless steel but not carbon steel.

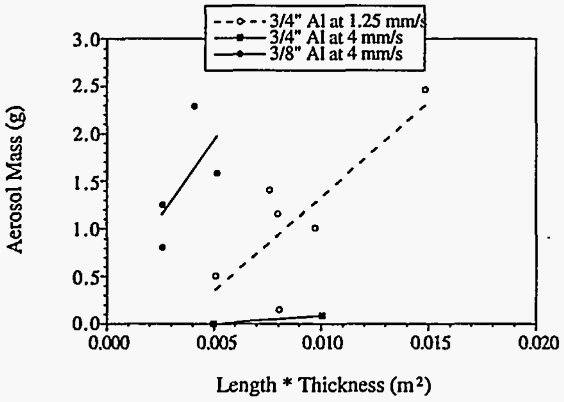

Figure 1. Aerosol mass produced as a function of the product of the cut length and plate thickness for 100 A torch currents.

The fact that the aerosol production appears to be a function of the material thickness, leads to a potentially serious problem in designing the user guide. To provide a reasonable estimate of aerosol production for a specified cut, that particular thickness of material would need to have a separate correlation. This would require significantly more work than originally expected and also require a much larger file size and memory for the user guide. The alternative is to provide the user with an estimate based on the correlation that provides the maximum expected aerosol for the particular cutting tool and material only. This method would keep the user guide to a more manageable size and still provide worst case estimates for risk assessments designing pollution control systems. The downside of this method is that the aerosol mass could be over estimated by an order of magnitude, resulting in a much greater expense due to overdesign of the particle capture system.

It was noted that as the cutting speed is increased the mass lost by the plate decreased and that as the cutting speed is increased the kerf width becomes narrower. Clearly, a smaller kerf width would correlate with less mass lost from the plate because a smaller kerf width implies a smaller volume of material removed from the plate by the cut. These observations are consistent with the explanation that higher energy inputs due to slower cutting speeds should result in wider kerfs and more material being removed from the plate. However, the increase in both kerf width and mass lost from the plate appear to increase linearly with decreasing cutting speed, in contrast to the peak observed in the aerosol production at slower cutting speeds.

The average particle size distribution for all of the tests done with aluminum is plotted in Figure 2. The average particle size distribution is weighted heavily towards the smaller particles. Approximately 85% of the mass distribution is found to be below 1 µm, indicating that the vaporization and recondensation of the aluminum is the dominant aerosol formation mechanism. In addition to the large peak in the submicron range, there is also a small peak around 10 µm due to the atomization of the molten metal. The average Mass Median Aerodynamic Diameter (MMAD) is 0.48±0.17 µm for the aluminum cuts.

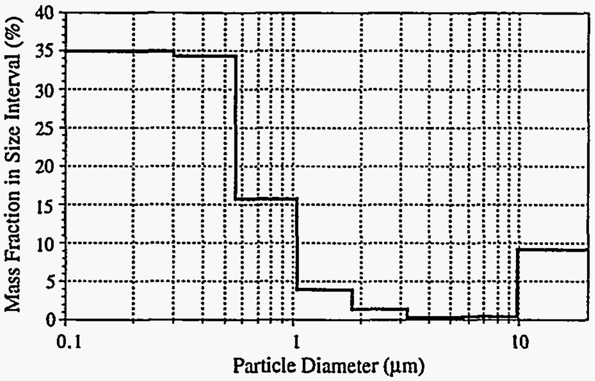

Figure 2. Average aerosol mass distribution as a function of particle diameter for 45 cascade impactor measurements of aluminum.

Carbon Steel

For carbon steel, a relatively shallow aerosol maximum is observed around 80 to 85 amps. This maximum aerosol production agrees with the maximum in mass lost by a plate, which is also peaks at plasma torch currents around 80 to 85 amps. The coincidence of the peaks in aerosol production and mass removed from the workpiece are in contrast to the linearly increasing response with aluminum. One possible explanation is that the thermal conductivity of carbon steel (1.0 J/s cm K) is only about a third that of aluminum (2.8 - 3.0 J/s cm K), therefore the higher local temperatures would be expected to result in larger kerf widths which reduce aerosol production.

For a fixed current of 80 amps, and again keeping the material thickness, gas pressure, tip size and torch height constant, a maximum in aerosol production was found to occur at a cutting speed of approximately 0.5 cm/s. As with aluminum, the peak in aerosol production as a function of cutting speed, was not matched by a corresponding peak in the mass of plate lost. However, the mass of plate lost from a cut does appear to peak at about 0.8 cm/s, which is reasonably close to the aerosol production peak at 0.5 cm/s. Whereas the mass lost from the aluminum plate did not peak for any of the cutting speeds tested.

Maintaining a constant plasma torch current of 80 A and a cutting speed of 0.5 cm/s, the cut lengths were varied between 5.0 cm to 91.3 cm on carbon steel thicknesses of 0.95 cm (3/8") and 1.9 cm (3/4"). The data from this series of cuts, as seen in Figure 3, resulted in an excellent correlation between the aerosol mass produced and the cut length x material thickness (R = 0.99). This single linear correlation for both thicknesses of carbon steel, is very different from multiple correlations required for different thicknesses of aluminum and stainless steel. There is no clear explanation for this phenomena at this time. It is also observed that the total aerosol production is much greater for carbon steel than for either aluminum or stainless steel for identical cutting parameters.

The kerf width was found to increase with increasing plasma torch current and decreasing cutting speeds. The carbon steel exhibited minimal warpage after cutting which enabled the kerf measurements to be easily made. The trend of increasing kerf width with arc current is consistent with trends noted by Bach[1]. The data also indicates that the MMAD decreases with increasing current and decreasing cutting speed. Both of these data sets are rather scattered, but of these observed trends are consistent with the energy model. More than 50% of the mass of aerosols produced by a cut are smaller than 1 μm. This implies that the vaporization and condensation mechanism is dominant over the atomization mechanism.

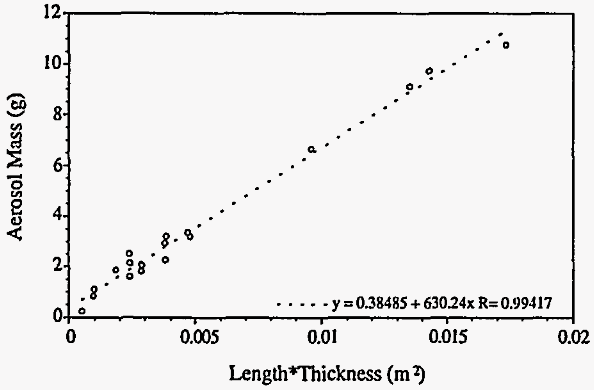

Figure 3. Aerosol mass produced by 80 A plasma torch cuts on carbon steel at 0.5 cm/s as a function of the product of the cut length and plate thickness.

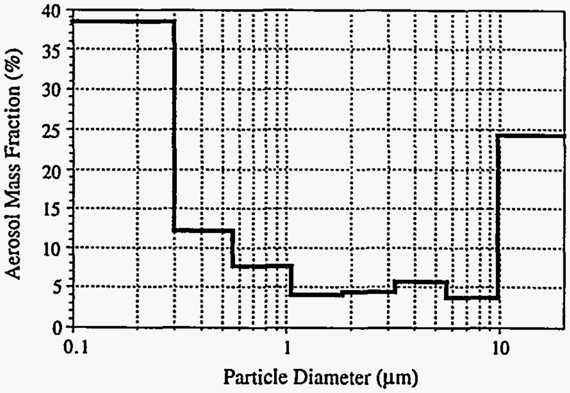

Figure 4. Average aerosol mass distribution as a function of particle diameter for 36 cascade impactor measurements of carbon steel.

Figure 4 is a histogram summarizing the average mass distribution of the aerosols collected by the cascade impactor for carbon steel. The two most common diameters containing most of the aerosol mass are above 9.8 μm and smaller than 0.30 μm. The average MMAD from all of the carbon steel cuts is calculated to be 0.52±0.12 μm and the range of MMAD's is from 0.26 μm to almost 3 μm. This bimodal characteristic underscores the caution that must be taken when either reporting or using a single quantity like the MMAD to describe an aerosol distribution. The MMAD is simply the mass median diameter, and is not indicative of the most common diameters that contain the majority of the mass.

Stainless Steel

The maximum aerosol production for stainless steel was found to occur at the upper limit of the plasma torch power supply. The mass lost from the plate also increased linearly as a function of current to the upper limit of the arc current. Fixing the plasma torch current at 100 A, the maximum quantity of aerosols produced was found to be at a cutting speed of 0.25 cm/s. This is a cutting rate of only about one half compared to the cutting speeds for aluminum and carbon steel. With the arc current held at 100 A and cutting speed at 0.25 cm/s, the length of cut and material thickness were varied. Figure 5 shows that, as with aluminum, the thinner piece of stainless steel produced more aerosols than the thicker piece.

The maximum quantity of aerosol produced was about 3.5 g for stainless steel, 3.2 g for carbon steel but only about 2.25 g for aluminum for equivalent 40 cm cuts. The fact that the aerosol mass produced from the stainless steel was greater than the aluminum, could be attributed to the greater amount of slag that was found on both the thin and thick plates of aluminum. Stainless steel generally showed little if any slag for most cuts except those that were cut too fast or at too low a current. It is believed that less slag translates into more aerosol because it means that the shear forces were sufficiently high to tear the liquid material from the plate. This process should favor additional droplet formation. In addition, the thermal conductivity of stainless steel (0.3 J/s cm K) is only one tenth the thermal conductivity of aluminum. This lower heat conductivity would result in higher temperatures at the kerf and hence greater aerosol production for stainless steel, as is demonstrated by this data.

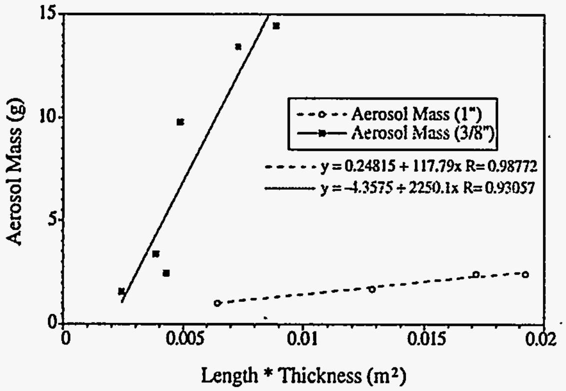

Figure 5. Aerosol mass collected from 100 A plasma torch cuts on 3/8" and 1" stainless steel plate at a cutting speed of 0.25 cm/s, as a function of the product of cut length and plate thickness.

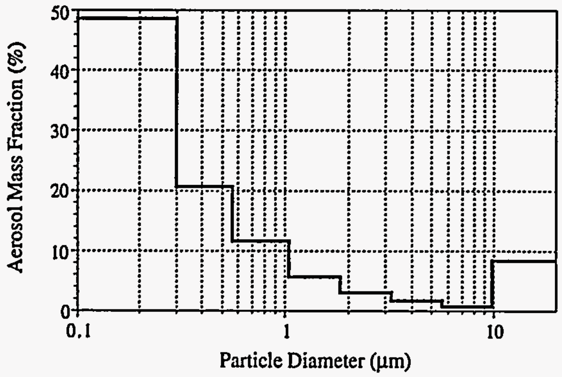

Figure 6. Average aerosol mass distribution as a function of particle diameter for 24 cascade impactor measurements on stainless steel.

The mass of plate lost increases linearly with decreasing cutting speed and does not match the maximum aerosol production peak. The stainless steel data indicates that an increase in the plasma torch current results in a larger kerf, as noted with the other materials tested. It is somewhat surprising, given the fact that the stainless steel exhibited a great deal of warping during a cut, that the data did not exhibit much scatter. Clearly, the warpage of the stainless steel during a cut was yet another uncontrolled variable that may have had some effect on the consistency of the results for stainless steel.

Figure 6 presents the average aerosol size distribution for 24 cuts on stainless steel. The distribution is similar to aluminum in that less than 15% of the aerosol mass is contained in particle sizes greater than 1 µm. The distribution of stainless steel particles results in the smallest median diameter (MMAD = 0.36±0.09 µm) of the three materials cut with the plasma torch.

FIELD SAMPLING TESTS

Experimental Description

The numerous laboratory experiments, previously described, have been conducted to determine the behavior and generation rates of aerosols in the cutting of metals, as a prerequisite to creating a database for the user guide. However, experiments carried out in the laboratory are under controlled conditions, whereas, conditions present in actual decommissioning processes are not. Many variables such the combination of different metals in a structure, the accumulation of paints, dust, dirt or some other deposits on the surface and human inconsistencies in freehand cutting, have not and cannot be easily taken into account in laboratory experiments. In addition to the inconsistencies present between laboratory and field cutting environments, cuts performed in the laboratory are conducted on a smaller scale that actual conditions. Since the length of the cuts performed in the laboratory are limited to the box enclosure, the cuts performed under actual conditions can be significantly longer than the ones performed in the laboratory. Therefore, it is necessary to test the extrapolation of the laboratory data in order to predict the aerosol generation amounts for longer field cuts. In this context, the field sampling tests have two main goals. The first is to provide a measure of the error that is inherent between the controlled laboratory tests and the more variable field tests. The second goal is to determine the validity of the empirical equations, developed in the laboratory tests, in extrapolating predictions for the field cuts.

The field sampling tests were conducted during the actual decommissioning of the EBWRII Reactor at the Argonne National Laboratory. Two types of torches, a plasma torch and an oxyacetylene torch, were used for the EBWRII decommissioning operations of a water retention tank and a number of stainless steel pipes. All cuts were performed in an enclosed canvas tent with exhaust ducts located near the ceiling of the containment tent. Ventilation was provided by a total of 473 m^3/s (1000 cfm) of air flow through two flexible 20 cm (8") diameter ducts. The aerosol particles generated by the cuts were collected by a prefilter and HEPA filter system at the end of the flexible ductwork. The field sampling apparatus was connected to one of the flexible ducts between the tent and the prefilter. The dimensions of the field sampling inlet was constructed to provide a sample gas velocity that was nearly identical to the gas velocity in the duct, to allow for isokinetic sampling. This ensured that the sampled aerosol was representative of the concentration and size distribution of the aerosol in the ductwork and, by reasonable assumption, the aerosol in the tent.

Carbon Steel Results

The first field sampling cuts were performed on a 4.6 m (15 ft) long, 3.0 m (10 ft) diameter cylindrical water retention tank fabricated from 1/2" thick carbon steel. Although most of the paint on the tank had been removed there was still some residual paint on the outside surface. In addition, there was also a glass lining on the inside surface of the tank that could not be removed prior to the cuts. The tank was cut using a manually operated oxyacetylene torch. Due to ambient temperatures above 38 C (100 F) inside the containment tent, cuts were performed by a rotating team of welders in 15-40 minute intervals. Five different HEPA filters used to obtain data for various cut lengths during the decommissioning of the water retention tank. The mass of aerosol collected as a function of the product of the length of the cut and the material thickness is plotted in Figure 7. A cascade impactor was used to determine the MMAD of the aerosol distribution. The results indicated that an MMAD of 0.25 µm was obtained for the glass lined carbon steel tank. Since the laboratory tests have been completed only for a plasma torch, no comparisons between field and laboratory data can be made at this time.

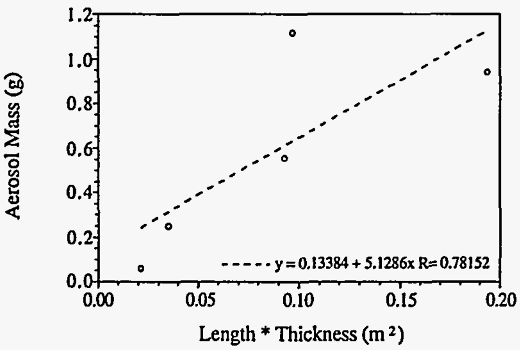

Figure 7. Aerosol mass produced during field cuts with an oxyacetylene torch on a 1/2" carbon steel, glass lined, water retention tank.

The field data are reasonably self consistent, showing a linear increase in aerosol mass with increasing cut length. The one exception is for the point with a cut length of 7.6 m (25 ft) where about twice as much aerosol mass was collected compared to a similar 7.3 m (24 ft) cut. It was observed that the cut performed for this test was conducted near the floor. It was also observed that there was considerable dust and dirt on the floor which was made airborne by the operation of the oxyacetylene torch. Finally, it was observed that the portion of the tank near the floor had the most residual paint remaining on the surface of the tank. It is quite possible that the reentrained dirt and burned paint combined to substantially increase the particle mass collected by the filter, explaining the unusual amount of aerosol mass collected for that one test.

Stainless Steel Results

Two field cuts were also monitored from a manually operated plasma torch on two 30 cm (12") diameter, schedule 40 stainless steel pipes. Each pipe was 1.8 m (6 ft) long with a wall thickness of 1.9 cm (3/4"). Since this field data was collected for plasma torch cuts on stainless steel, some comparisons can be made with the laboratory data. However the scope of the conclusions are necessarily limited due to only two data points.

Impactor measurements made on one of the cuts resulted in a measured MMAD of 0.26 µm. This single measurement is in reasonable agreement with the average of the 24 laboratory size measurements of 0.36±0.09 µm. The aerosol mass collected from the two field cuts is included for comparison with all of the laboratory stainless steel data in Figure 8. The two data points on the far right hand side of the graph represent the field samples. Two curve fits are shown in the plot. The upper curve is based on the maximum aerosol measured in the laboratory for 100 A cuts on 0.95 cm (3/8") stainless steel plates at a cutting speed of 0.25 cm/s. The lower curve was the quantity of aerosol measured using the same cutting parameters on 2.54 cm (1") thick plates. As discussed earlier, these cutting parameters do not maximize the aerosol when used on larger thicknesses. In fact the lower curve is very near the slope of a curve that is fit to all of the laboratory data. Therefore, the two curves define the maximum aerosol and the average aerosol productions. Clearly, one field sample point is quite close to the average mass of aerosol that might be expected based on the laboratory data, while the other is just slightly less than the maximum expected from the laboratory data.

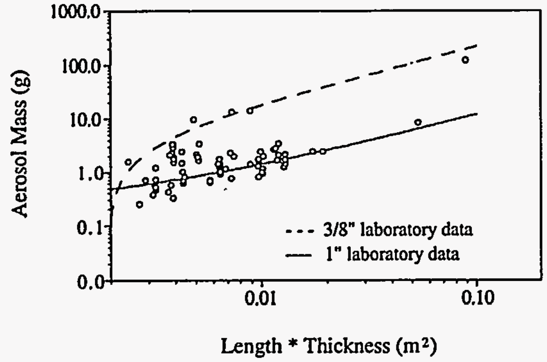

Figure 8. Two field data points (far right) from plasma torch cuts on stainless steel pipe, combined with all stainless steel laboratory data. Upper curve is fit through 3/8" laboratory data, lower curve is fit through the 1" laboratory data.

CONCLUSIONS

Aerosol production from plasma torch cuts has been characterized for a variety of operational parameters. Most of the observations and data trends can be explained using simple energy considerations. Unfortunately, the simple model cannot quantitatively predict aerosol or total waste production. Empirical correlations for a certain specific sets of test conditions can be used to predict the quantity of particulates produced to within ±50%. However, setting up a test program to derive a correlation for all possible variables does not appear to be realistic. The major problem is to account for the thickness of the material. For carbon steel, the thickness can be normalized and the data can be fit with a single line. This allows predictions to be made to within ±10% regardless of the plate thickness. Aluminum and stainless steel would require separate correlations for each thickness to achieve a similar accuracy. Therefore, it appears that the simplest solution is to determine a correlation for the worst case scenario of particle production. Preliminary field tests have shown that using the worst possible prediction based on laboratory data, encompasses the range of field measured data

Therefore, it seems feasible to construct a user guide that combines a database of cutting information with a calculational program to provide an extensive compilation of cutting experiences, and to furnish a D&D project with guidelines in terms of predicting total aerosol production, aerosol generation rates, suggested tool operating settings, and the minimum HEPA filtration area necessary to contain the expected aerosol release. D&D contractors, planners, and ES&H personnel would use this information in conjunction with the specifics of the application, and site specific safety guidelines to determine the appropriate cutting tool for the job, and the necessary pollution controls required, including filtering, personal protection, and air monitoring.

REFERENCES

1. Bach W., H. Steiner, G. Schreck, and G. Pilot, "Analysis of Results Obtained with Different Cutting Techniques and Associated Filtration Systems for the Dismantling of Radioactive Metallic Components." Commission of European Communities, Report EUR14213, (1993).

2. T. Nishizono, Y. Ikezawa, "Characteristics of Aerosol Generated during the JPDR Decommissioning," Proceeding of the 12th ISCC in Yokohama, (1994)

3. W. Bach and A. Gruchow "Plasma Cutting in Atmosphere and Under water" Pure and Applied Chemistry, V. 64, No. 5, pp. 665-670, (1992).

4. K.H. Schaller, B. Huber, *Decommissioning of Nuclear Power Plants*, Graham & Trotman Ltd., (1984).

5. Newton, G., M. Hoover, E. Barr, B. Wong, and P. Ritter. "Collection and Characterization of Aerosols from Metal Cutting Techniques Used in Decommissioning Nuclear Facilities," American Industrial Hygiene Association Journal, Vol. 48, pp. 922-932 (1987).

6. H. Deipenau, H. Osterlitz, Fr.-W. Bach: Anwendung des Pulver- und Plasmaschmelzschneidens auf die Demontage von Kernkraftwerken bei Stillegung BMFT RS 0274/7 (1981)

7. R Leautier, G Pilot, A Calvet, A Langonnet, G Michael, H Loyer, P Morel Decommissioning of Nuclear Installations - Under Water Plasma Arc Cutting CEC Programme on the decommissioning of nuclear installations Contr. No. FI 1 D 0037 progress report 4.

*Work supported by the United States Department of Energy, Nuclear Group, under contract W-31-109-ENG-38

DISCLAIMER

This report was prepared as an account of work sponsored by an agency of the United States Government. Neither the United States Government nor any agency thereof, nor any of their employees, makes any warranty, express or implied, or assumes any legal liability or responsibility for the accuracy, completeness, or usefulness of any information, apparatus, product, or process disclosed, or represents that its use would not infringe privately owned rights. Reference herein to any specific commercial product, process, or service by trade name, trademark, manufacturer, or otherwise does not necessarily constitute or imply its endorsement, recommendation, or favoring by the United States Government or any agency thereof. The views and opinions of authors expressed herein do not necessarily state or reflect those of the United States Government or any agency thereof.